# Nonlinear Model Reduction for Control of Distributed Systems: a Computer-Assisted Study

**Stanislav Y. Shvartsman and Ioannis G. Kevrekidis**
Dept. of Chemical Engineering, Princeton University, Princeton, NJ 08544

*Model reduction methodologies for the partial differential equations modeling distributed parameter systems constitute an important first step in controller design. A systematic computer-assisted study illustrating the use of two such methodologies (Approximate Inertial Manifolds and the Karhunen-Loève expansion) in controlling (stabilizing) a nonlinear reaction-diffusion problem is presented. The approximation quality of the models, issues of computational implementation of the reduction procedure, as well as issues of closed-loop stability are addressed.*

## Introduction

If sound first-principles models of an engineering process are available, it makes sense to exploit them for controller design (e.g., Henson and Seborg, 1996). Advances in scientific computation have increased the level of fundamental understanding that can be built into such models and, as a result, their realism and predictive power. As the models of distributed-parameter systems (DPS) become more sophisticated and spatially resolved, so do contemporary sensing capabilities: the rapid development of imaging techniques allows one to visualize (and thus feedback) in real time information about the spatiotemporal state of the system (Rotermund et al., 1990; Flaetgen et al., 1995, Brown et al., 1985; Qin and Wolf, 1996). While the logical path "physical process model–controller design" is conceptually clear (Henson and Seborg, 1996; Bequette, 1991; Kravaris and Kantor, 1990; Ogunnaike and Ray, 1994), its implementation is not at all straightforward. The corresponding controller design problem becomes progressively more complicated as the size of the dynamical system increases (Boley, 1994). Discretizing the underlying conservation laws (in most cases partial differential equations (PDEs)) gives rise to dynamical systems of a very high order. Large size is also a problem when it is necessary to simulate the process model "on-line," for example, for estimation purposes or while solving sequential open-loop optimization problems in a model predictive control formulation (Meadows and Rawlings, 1994).

The approach traditionally used in chemical engineering to address problems of control and estimation in distributed-parameter systems is based on using finite (but not too large) discretizations of the underlying PDEs. This has been illustrated in the treatment of problems such as the distributed observer design for heat and mass-transfer processes (Ajinkaya et al., 1975; Koda and Seinfeld, 1982; Marquardt and Auracher, 1990) or the control of unstable steady states in fixed-bed reactors (Georgakis et al., 1977; McDermott and Chang, 1984; Bonvin et al., 1980). Recent examples of using such moderate-size discretizations to control nonlinear, pattern-forming reacting systems can be found in Dainson and Sheintuch (1997) and Karafyllis et al. (1997). More recently, however, there has been intense interest in controlling problems whose models have significantly higher complexity, necessitating discretizations of much higher order. Such problems include semiconductor manufacturing reactors (e.g., Badgewell et al., 1994; Aling et al., 1997), reverse-flow and circulating-loop reactors (e.g., Nieken et al., 1994; Hua et al., 1998), control of transitional hydrodynamic flows (Joshi et al., 1997; Carlson and Lumley, 1997), or instabilities in turbines (Badmus et al., 1996; Paduano et al., 1994). Problems with complicated geometries and/or sharp variations of solutions or system parameters make the use of larger discretization models unavoidable (Aling et al., 1996; Aling et al., 1997; Bangia et al., 1997; Graham et al., 1993; Chakravarti et al., 1995). Thus, it is important to reduce the physically based models to incorporate them in existing control methodologies.

Tools for accurate model reduction play an important role in bridging realistic model development with model-based control techniques. The dissipative nature of the partial differential equations underlying reaction and transport processes make the large-scale dynamical systems arising in the discretization of these PDEs *effectively* low-dimensional. This, loosely speaking, means that the long-term dynamic behavior

is characterized by a small number of active degrees of freedom.

In this article we attempt to use methods of low-dimensional modeling of large-scale dynamical systems for feedback control. We (among others) have successfully used such methods in studies of open-loop stability and dynamics of distributed parameter systems such as grooved-channel flow, reaction-diffusion systems, rapid thermal processing, and a variety of model problems (Deane et al., 1991; Graham and Kevrekidis, 1996; Aling et al., 1997; Bangia et al., 1997). As the sophistication of sensor and actuator technology develops, issues of real-time identification for DPS (e.g., Rigopoulos et al., 1997) and its interaction with model reduction (Gay and Ray, 1995) and controller design (see the discussion in Banks et al., 1997) become increasingly important. PDE-based control of distributed parameter systems is quite developed for complex mechanical systems, (e.g., large mechanical structures, Bansenauer and Balas, 1995) where the models are firmly established. In reaction/transport systems the models are, as a rule, not so well defined. Nevertheless, developments in modeling and computation, as well as in spatially resolved sensing techniques, are already making PDE-based control possible (see, for example, the experiments in Qin and Wolf (1995) and Petrov et al. (1997)).

The article is organized as follows: First we discuss issues associated with the role of model reduction in the design of finite-dimensional controllers for DPS. We then briefly introduce our illustrative example (a nonlinear reaction-diffusion system) and the associated stabilization problem. The fourth section is dedicated to the description of model-reduction methods we use in this article to obtain the low-dimensional vectorfields used in controller design. In the fifth section a computer-assisted study of the closed-loop dynamics and stability of the resulting feedback systems is presented, and we conclude with a discussion and comments motivated by our observations.

## Approaches to Model Reduction

The temporal evolution of many dissipative DPS of engineering interest is governed by partial differential equations and the *state* in the corresponding control problem is infinite dimensional. The discrete nature of actuators, however, as well as finite precision and limited memory capacity of computers implementing control action, necessitate the discretization (lumping) of the DPS to a finite-dimensional dynamical system (Ray, 1981; Balas, 1979; Sakawa, 1983; Curtain, 1985). The good approximation of the dynamics of the original, infinite-dimensional system by the discretized (lumped) one is the subject of ongoing research (Témam, 1988; Constantin et al., 1988). A very important argument for the quantitative validity of this approximation is the *dissipative* nature of the PDEs. The spectrum of the linear (or linearized) part of the evolution equations has the form illustrated in Figure 1: here the open-loop spectrum is bounded on the right and contains only a finite number of unstable eigenvalues. This suggests that the long-term dynamics is low-dimensional and that, therefore, a finite-dimensional controller may be designed that would "take care" of the least stable modes only. This form of the spectrum is typical for problems dominated by diffusion, heat conduction, and/or

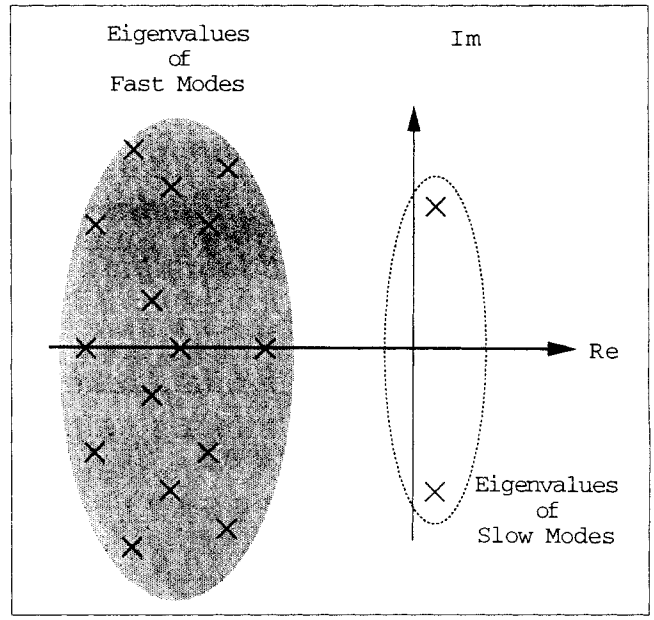


**Figure 1. Spectrum of the linearization of a dissipative nonlinear DPS around a nominal steady state.**

Typical features: boundedness on the right, finite number of unstable modes, increasing "spectral gaps" between stable eigenvalues.

viscosity, a class that encompasses reaction-diffusion systems, packed-bed reactors at moderate Péclet numbers, rapid thermal processing units, and many other systems of engineering interest (Ray, 1981).

In some cases, extensive experimental and modeling experience with a process can guide the construction of low-dimensional, control-relevant models backed up by good physical understanding of the underlying dynamics (such as the traveling-wave models for distillation columns and packed-bed reactors, Doyle at al., 1996). In general, discretization methods (finite difference, finite-element, spectral, etc.) yield finite-size dynamical systems; using existing control methodologies it is conceptually straightforward to synthesize finite-dimensional controllers for any of these dynamical systems. The important question then is whether it is possible to control the infinite-dimensional system with such a finite-dimensional controller. A positive answer (for linear systems) can be found in a definitive sequence of articles written over the last 20 years by Balas, Curtain, Sakawa, and others (Balas, 1979, 1980, 1982, 1983, 1985; Curtain, 1985; Sakawa, 1983). The issue of *stabilization* of DPS by finite-dimensional controllers was addressed by Balas, motivated mainly by control of large-scale mechanical structures. Provided that the size of the reduced-order model is large enough, the stability of the combined DPS and finite-dimensional controller is proved for linear [e.g., Balas (1982)], and some classes of nonlinear [Balas (1991)] PDEs; the controller should be based on a sufficiently "converged" discretization of the DPS. Sufficiently converged discretizations, while finite, will routinely be large dynamical systems (from $O(10^2)$ for one-dimensional problems to several millions of unknowns for three-dimensional problems in space); the routine design of controllers for such problems has difficulties of its own. High-order and ill-conditioning, for example, might render the corresponding linear control prob-

lems "Riccatti unsolvable" (Su and Craig, 1991), and special numerical techniques are necessary to assess basic properties of the linearized state-space models, such as controllability, stabilizability, and observability (Boley, 1994).

A second reduction problem therefore arises: Is it possible to control these converged discretizations with a finite-dimensional controller, based on a (much smaller) accurate reduced model? The language of Balas's and other (Curtain, 1985; Sakawa, 1983) articles on stabilization of infinite-dimensional systems with controllers based on reduced models is that of Hilbert spaces and infinite-dimensional dynamical systems. Fortunately, the same line of thought and terminology also applies in understanding potential sources of instabilities in this second reduction problem. In this article we are concerned precisely with this problem: the control (in our case, stabilization) of large, converged discretizations of DPS with controllers designed using *smaller but accurate* vector-fields. In both cases the crucial stability issue comes from the interaction of the finite-dimensional controller, based on the "small" reduced-order model, with the dynamics of the residual modes (those neglected at the controller design stage). For linear systems it is possible to obtain analytical expressions for the degree of destabilization caused by control spillover of energy to residual modes and by dynamic coupling of retained and residual modes (Balas, 1982a). Large-scale scientific computation (iterative techniques for large eigenproblems) have been recently combined with analytical results from the perturbation theory of spectral operators to perform algorithmic stability checks on closed-loop infinite-dimensional systems with low-order controllers of this nature (Erikson and Laub, 1995) (see also Haczyc and Palazoglou (1991) for the so-called eigenvalue inclusion technique for assessing closed-loop stability).

To illustrate the basic issues related to stabilization of large state-space models by finite-dimensional controllers of smaller size, consider the control problem for a large finite-dimensional linear system (ROM1).

$$\dot{x} = Ax + Bu. \tag{1}$$

The conventional approach to low-order controller design involves identification of a (small) set of modes critical for the system dynamics, and projection of the original problem onto the low-dimensional subspace spanned by these modes. The state $x \in R^n$ is split into $x_1 \in R_1$ and $x_2 \in R_2$, ($R^n = R_1 \oplus R_2$, $\dim(R_1) = m$, $\dim(R_2) = n - m$, $m \ll n$). $R_1$ is the subspace spanned by the "critical" (the least stable) modes, while $R_2$ is its orthogonal complement:

$$\dot{x}_1 = A_{11}x_1 + A_{12}x_2 + B_1u \tag{2}$$

$$\dot{x}_2 = A_{21}x_1 + A_{22}x_2 + B_2u. \tag{3}$$

Here $A_{11}, A_{12}, B_1$, and so on are blocks of the matrix representation of operators $A$ and $B$ transformed to the basis formed by the critical modes and their orthogonal complement. Ignoring the components in the residual subspace (truncating), the control problem (e.g., selection of a stabilizing matrix of gains $K$ in the case of the full-state feedback) for the resulting low-order model (ROM2) is solved as follows

$$\dot{x}_1 = (A_{11} - B_1K)x_1 \tag{4}$$

and the stability of the resulting closed-loop system,

$$\dot{x}_1 = (A_{11} - B_1K)x_1 + A_{12}x_2 \tag{5}$$

$$\dot{x}_2 = (A_{21} - B_2K)x_1 + A_{22}x_2, \tag{6}$$

including the unmodeled dynamics, is then examined. Several comments are in order (Balas, 1979):

- Since $B_2$ is in general nonzero, the controller stabilizing ROM2 will influence the dynamics of the residual modes (control spillover).
- When the matrix of $A$ in ROM1 is diagonal, the closed-loop matrix will be block triangular and the high-order closed-loop system will be stable. For nonzero $A_{12}$ and $A_{21}$, there will be dynamic coupling between the $x_1$ and $x_2$ components of the state (modeling error).

Critical modes can be chosen in different ways: they can be the exact eigenvectors of a linearized problem, corresponding to the leading part of the spectrum (Bansenauer and Balas, 1995), their Krylov subspace approximations (Hsu and Vu-Quoc, 1996), or empirically determined eigenfunctions (POD modes, see the third section). Clearly, the *truncated* problem (ROM2) must accurately approximate the open- and closed-loop dynamics; the accuracy of the reduced-order model is related to the norms of the neglected off-diagonal blocks of the full Jacobian.

The accuracy of approximation might be improved by making the low-order model "aware of the residual dynamics" (Kokotovic et al., 1986; Balas, 1982a,b). This path is especially clear when the original system is of the form

$$\dot{x}_1 = A_{11}x_1 + A_{12}x_2 + B_1u \tag{7}$$

$$\mu\dot{x}_2 = A_{21}x_1 + A_{22}x_2 + B_2u, \tag{8}$$

where $\mu \ll 1$ is a small parameter. In this case (Kokotovic et al., 1986), one can obtain a slaving relationship between the residual (*slaved*) and critical (*master*) modes

$$x_2 = S(x_1; u; \mu). \tag{9}$$

Methods of singular perturbation theory allow the construction of such slaving functions (invariant manifolds) to any given accuracy. For the linear system (7,8) the $O(\mu)$ approximation of such a manifold is given by

$$x_2 = -A_{22}^{-1}(A_{21}x_1 + B_2u). \tag{10}$$

The "corrected" low-order model becomes

$$\dot{x}_1 = A_0x_1 + B_0u \tag{11}$$

$$A_0 \equiv A_{11} - A_{12}A_{22}^{-1}A_{21}, \qquad B_0 \equiv B_1 - A_{12}A_{22}^{-1}B_2. \tag{12}$$

The fundamental robustness result given in Kokotovic et al. (1986) ascertains the stability of the full system with a controller (full-state feedback) designed based on $A_0$, $B_0$, feeding back the *slow* component of the state only. This is especially important since the fast components of the state will in

general be difficult to measure/estimate and consequently to feedback. Kokotovic et al. (1986) and Kokotovic and Sauer (1989) have extended the tools of invariant manifolds for controller design in nonlinear systems as well. Their work leads to dimensionality reduction of the closed-loop system; they design *composite* feedback control, decomposing the input into two parts "addressing" the slow and fast dynamics of the system separately.

In the infinite-dimensional context (PDEs) *inertial* manifolds—smooth, invariant, globally attracting, finite-dimensional manifolds—become an important tool in model reduction for control purposes. While the solution lives in an infinite-dimensional function space, the long-term dynamics is often contained on a finite-dimensional, smooth (Lipschitz), exponentially attracting manifold (Foias et al., 1988b); this manifold can be parameterized by a finite number of modes ("master modes" in the preceding discussion). These manifolds are global in phase space and can therefore be thought of as generalizations of center manifolds (Guckenheimer and Holmes, 1983). Open-loop low dimensionality suggests that (for the appropriate class of feedback laws) closed-loop low dimensionality will prevail; more importantly, the closed-loop inertial manifold can be expected to be parametrized by the same modes as the open-loop one. Thus, the theoretical tools for construction of inertial manifolds, and their numerical counterparts for the construction of approximate inertial manifolds (AIMs), may be incorporated in the formulation of the vectorfields describing closed-loop dynamics. In particular, these vectorfields can be used in the design of feedback controllers. As the theory of inertial and approximate inertial manifolds developed in the last decade (Foias et al., 1988a; Jolly et al., 1990) a number of researchers started exploiting its utility for DPS controller design.

Brunovsky suggested the use of inertial manifold techniques for prescribing the low-dimensional dynamics in the closed-loop (Brunovsky, 1991). Recently, Sano and Kunimatsu proved the existence of a closed-loop invariant manifold in a nonlinear diffusion equation, along with designing a finite-dimensional stabilizing controller based on the AIM-reduced dynamics (Kunimatsu and Sano, 1994; Sano and Kunimatsu, 1994). In the chemical engineering literature Chen and Chang (1992) used tools of center manifold and normal form theory to design a nonlinear controller and obtain the closed-loop center manifold for a truncated DPS; in their case proximity to a bifurcation guaranteed the separation of relevant time scales (i.e., the presence of a small parameter) in the problem. They also exploited empirical eigenfunctions in identifying approximations of the leading linear modes of an unknown DPS for feedback purposes. Daoutidis and Christofides have gone beyond the finite-dimensional singular perturbation work of Kokotovic et al. (1986, 1989) to exploit invariant manifolds in the infinite-dimensional case (Christofides and Daoutidis, 1996, 1997; Christofides, 1997). Using singular perturbation methods, they designed observer-based nonlinear feedback controllers (through the corresponding closed-loop AIMs) and demonstrated their performance.

Even when the existence of inertial manifolds can be theoretically ascertained, their practical computation and use involves a certain degree of approximation. The selection of spatial modes used to parametrize the manifold, the choice of the number of parametrizing "master" modes, and of the residual "slaved" ones, as well as the particular method of approximating the slaving function must be addressed. Most of the analytical and initial numerical work has been in cases where the manifold was parametrized by Fourier modes (e.g., trigonometric, Chebyshev, or Legendre polynomials: Jolly et al., 1990; Graham et al., 1993; Shen and Témam, 1995). For problems with spatially dependent parameters and complicated geometries, however, the use of Fourier modes may be inconvenient or just impossible. Different global modes should then be chosen for parametrization of the manifold, such as numerically computed eigenvectors of a linear or linearized part of the problem (Batcho and Karniadakis, 1994; Hsu and Vu-Quoc, 1996) or empirical eigenfunctions (Deane et al., 1991; Bangia et al., 1997). It is important to note that additional AIM implementations based on finite difference, finite-element, and other numerical discretization techniques are also being pursued (Foias and Titi, 1991; Marion and Témam, 1990; Chen and Témam, 1993; Ammi and Marion, 1994).

In this article we present a comparative study of several derivations of reduced-order vectorfields for a nonlinear, one-dimensional in space reaction-diffusion system. Their utility for controller design is examined through a computational study of the stabilization problem.

## Problem Statement

In selecting a "minimal" but still truly illustrative example, we chose a one-dimensional DPS with strong nonlinearity (evidenced by several stable, coexisting patterned stationary states). Because model reduction is a crucial component of our study, the problem is such that "naive" low-dimensional approximations (say, a two-mode Fourier truncation) are very inaccurate; the sharpness of the spatially structured profiles of the system solutions renders such simple reductions useless. We chose to work on the stabilization problem for some of the nonlinear steady states of our model. While this is the simplest control objective, we believe it is a good starting point for systematically obtaining *quantitative* performance characteristics, such as prediction of the closed-loop dynamics and bifurcations, or success in low-dimensional pole-placement controller design.

### *Open-loop system*

The reaction-diffusion system constituting our example is described by a pair of coupled parabolic partial differential equations, known as the FitzHugh-Nagumo model (FitzHugh, 1962) with no-flux boundary conditions. This system (arising originally in neurophysiology) and its variants are often used to study issues of pattern formation in reacting systems, ranging from Belousov-Zhabotinsky and Chlorite-Iodide-Malonic-Acid reactions, to low- and high-pressure heterogeneous catalytic reactors (e.g., Imbihl and Ertl, 1995; Sheintuch and Shvartsman, 1996):

$$v_t = \Delta v + f(v,w) = \Delta v + v - v^3 - w \tag{13}$$

$$w_t = \delta\Delta w + g(v,w) = \delta\Delta w + \epsilon(v - p_1 w - p_0) \tag{14}$$

$$v_z|_{0,L} = w_z|_{0,L} = 0. \tag{15}$$

In these equations $v$ is usually termed the "activator" and $w$ the "inhibitor"; $\delta$ is the ratio of diffusivities of the two reacting species, while $\epsilon$ represents the ratio of time scales for the kinetic terms; $L$ is the length of the system box; and $p_1, p_0$ are parameters determining local dynamics. Considerable insight in the spatiotemporal dynamics accessible to such a system can be gained from a phase-plane analysis of the reaction terms by observing the two nullclines (the loci of points $v$, $w$ such that $f(v,w)=0$ and $g(v,w)=0$, respectively). Depending on the parameters $p_1$ and $p_0$ these nullclines can have a different number of intersections (steady states). Figure 2a shows the case when three intersections (and therefore three spatially uniform solutions, flat profiles in Figure 2b) exist. The interaction of the nonlinear reaction term with transport (diffusion) results in a large number of additional nonuniform steady states. These, for parameter values as in the plot in Figure 2a, may take the form of relatively sharp spatial concentration fronts separating the ignited (up) and extinguished (down) regions of the one-dimensional system. The wavelength of these nonuniform patterns may vary. Many nonuniform steady states coexist for a wide region of the system parameter space. The most clear-cut demonstration of such rich steady-state structure in an experimental reactor was provided by Luss and coworkers (Liauw et al., 1997; Somani et al., 1996).

Structured states may lose stability as the system parameters vary. The work of Meron and Hagberg (1994) presents the most detailed recent study of stability of fronts in the FitzHugh-Nagumo system. We illustrate some of the possible transitions by computing the bifurcation diagram associated with a particular front solution (thick line in Figure 2b). For low values of $\epsilon$ the spatially nonuniform solution is stable and appears as a front positioned approximately in the middle of the domain (upper inset in Figure 2c). The extinguished portion of the profile expands to the right as $\epsilon$ is increased, and at $\epsilon \approx 0.9445$ the front undergoes a saddle-node bifurcation—the branch turns around and for a wide range of $\epsilon$ values two-front solutions—a saddle and a node (the full and broken lines, respectively) coexist. At low values of $\epsilon$ the stable stationary front undergoes a Hopf bifurcation (Figure 2d) resulting in a spatiotemporal oscillatory solution, during which the front moves back and forth in space as time evolves. Projection of this limit cycle on the plane of zeroth Fourier modes (spatial average, $\langle\ \rangle$) of $v(z)$ and $w(z)$ is shown in Figure 2e.

### *Stabilization problem*

In this work we address the problem of stabilization of structured steady states, of the type described in the previous subsection. In particular, we focus on stabilization of solutions with low-dimensional instabilities (a small number of unstable eigenvalues). Two examples are shown in Figure 3; a single unstable eigenvalue (Figures 3a, 3b, 3e) and a single unstable complex eigenpair (Figures 3c, 3d, 3f). Spatiotemporal motions resulting from these instabilities are shown in Figures 3e and 3f. In the case of an unstable steady state beyond the (supercritical) Hopf bifurcation, infinitesimal perturbations lead to the development of a stable oscillatory front pattern; in the case of saddle-front solution, the perturbation shown leads, after a transient, to a distant (extinguished) steady state. By solving the stabilization problem we would like to maintain the reaction diffusion system at its open-loop unstable steady state by affecting the eigenstructure of its linearization. We assume that control enters additively into the nonlinear PDE, that the full state is available for feedback (thus sidestepping, for this work, estimation issues), and that feedback is implemented through manipulation of the amplitudes $u_j$ of finitely many ($s$) actuators with spatially nontrivial influence functions $q_j(z)$:

$$v_t = \Delta v + f(v,w) + \sum_{j=1}^{s} u_j q_j(z) \tag{16}$$

$$w_t = \delta \Delta w + g(v,w). \tag{17}$$

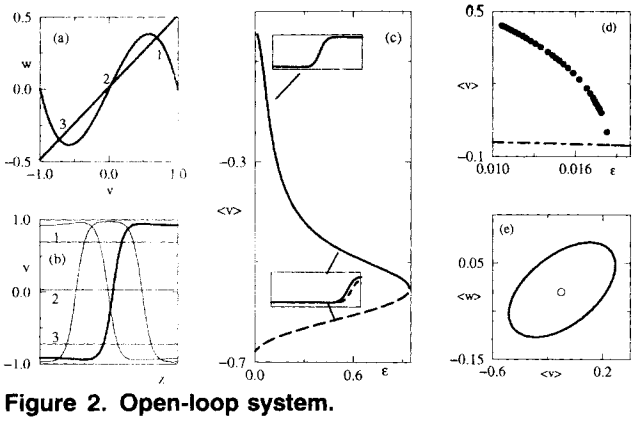


**Figure 2. Open-loop system.**

(a) Nullclines $f(v,w)=0, g(v,w)=0$ for $p_0=-0.03$, $p_1=2.0$. (b) Some of the steady states computed for $L=20.0$, $\epsilon=0.017$, $\delta=4.0$. (c) Steady-state bifurcation diagram for the front steady solution (thick line in (b)). The insets show the evolution of the profile with increased $\epsilon$. (d) Bifurcation diagram close to the Hopf bifurcation of the front at low values of $\epsilon$, ● denotes the resulting amplitude of the stable limit cycle. (e) Projection of the resulting spatiotemporal limit cycle and the unstable steady state surrounded by it on the plane of $(\langle v\rangle, \langle w\rangle)$.

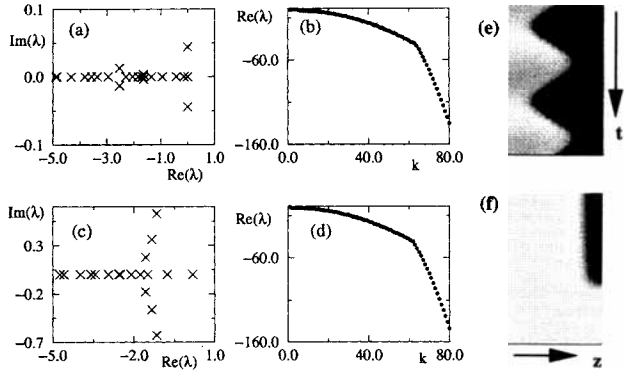


**Figure 3. Open-loop unstable set points.**

(a, c) Leading part of the spectrum of the linearization around representative open-loop unstable steady states corresponding to the front beyond the (supercritical) Hopf and before the saddle-node bifurcations, respectively. (b, d) Real parts of the eigenvalues of these steady states plotted vs. eigenvalue number, illustrating the strong dissipativity of the system. (e) Space–time plot of a limit cycle after the Hopf bifurcation (grayscale corresponds to the level of $v$). (f) Space–time plot of transient evolution away from an unstable, saddle-type front solution; the transient eventually approaches a spatially uniform "extinguished" steady state.

This form of an input (which physically would correspond to addition of material, and which is admittedly ad hoc) would smoothly approximate an input with compact support (a "zone feed" of material).

## Tools for Model Reduction

The two techniques we use in this article to effectively reduce the "large, converged Galerkin" to a small but accurate dynamic model for controller design purposes are based on (a) the theory of approximate inertial manifolds, and (b) the method of empirical orthogonal eigenfunctions (also termed proper orthogonal decomposition and Karhunen-Loève expansion). In this section we briefly describe the implementation of these techniques to obtain reduced open-loop vector fields for our problem, and compare the bifurcation diagrams of these vectorfields with those of the large, converged Galerkin vectorfield, which, for brevity, we will refer to from now on as "the full model." For each method we also point out the modifications necessary in the implementation to account for the actuators. The resulting reduced nonlinear vectorfields are later linearized around the nominal set point (open-loop unstable steady state) to yield state-space models used for controller design.

### *Approximate inertial manifolds*

Consider the abstract evolution equation

$$dr/dt + Ar + F(r) = 0, \tag{18}$$

where the infinite-dimensional state $r$ lies in a Hilbert space $r(z) \in H$. Assume that the leading linear term $A$ has a spectrum consisting of positive eigenvalues $\lambda_1 \le \lambda_2 \le \cdots$ and a complete orthonormal set of eigenfunctions $\phi_i$. For our reaction-diffusion example we take $A = -(\partial^2/\partial z^2)$ and define $F$ by the remaining terms. Assume that the solution can be accurately approximated by a "large" $n$-mode truncated Fourier series $r_n \in H_n = \text{span}\{\phi_i\}_{i=1}^n$

$$r \approx r_n = \sum_{i=1}^{n} r_i(t)\phi_i(z). \tag{19}$$

Using orthogonality of the basis functions $\phi_i$ we can uniquely split $r_n$

$$r_n = r_p + r_q, \tag{20}$$

where $r_p \in P_p H_n = \text{span}\{\phi_i\}_1^p$, $r_q \in Q_p H_n = \text{span}\ \{\phi_i\}_{p+1}^n$. $P_p$ and $P_n$ are orthogonal projectors onto the span of first $p(n)$ Fourier modes, respectively, while $Q_p = P_n - P_p$. A Galerkin weighted residual procedure results in a coupled system of $n$ equations describing the (joint) evolution of $r_p$ and $r_q$

$$dr_p/dt + Ar_p + P_p F(r_p + r_q) = 0 \tag{21}$$

$$dr_q/dt + Ar_q + Q_p F(r_p + r_q) = 0. \tag{22}$$

Setting $r_q = 0$ leads to the order $p$ (flat) Galerkin approximation of the original evolution equation

$$dr_p/dt + Ar_p + P_p F(r_p) = 0. \tag{23}$$

Figure 4 shows the branch of stationary fronts computed with Galerkin truncations of increasing order. We observe spurious saddle-node bifurcations present for low truncation orders, which disappear for finer discretizations (higher truncations). A way of improving the accuracy of approximation (without increasing the size of truncation) is the so-called nonlinear Galerkin method (Jauberteau et al., 1989), in which amplitudes of higher modes in the expansion are slaved to the amplitudes of the lower modes

$$r_q = S(r_p). \tag{24}$$

Note that $S = 0$ is the standard (flat, linear) Galerkin truncation. The rationale behind employing such slaving is based on the time-scale separation (the spectral gap) between dynamics of the master (slow, low wave number) and the slave (fast, high wave number) modes. For our example of a diffusion operator $A$ with boundary conditions leading to trigonometric Fourier series expansions, the $k_i^2$ factor resulting from the action of the linear operator $A$ on a mode with wavenumber $k_i$ substantiates this time-scale separation. Under the assumption that the partial differential evolution equation possesses an inertial manifold of dimension $p$ (which is represented as the graph of a function $S_\infty$: $P_p H \to (I - P_p H)$, and for our large truncation $S$ : $P_p H_n \to Q_p H_n$ we can write the approximate inertial form (AIF),

$$dr_p/dt + Ar_p + P_p F(r_p + S(r_p)) = 0. \tag{25}$$

Several methods have been proposed for the construction of contraction mapping algorithms for the computation of AIMs (and the corresponding AIFs). The so-called steady manifold (Foias and Témam, 1988), defined by the algebraic equations

$$Ar_q + Q_p F(r_p + r_q) = 0, \tag{26}$$

gives rise to a family of $\Phi$ maps (that are essentially consecutive steps in the successive substitution approximation of the steady manifold)

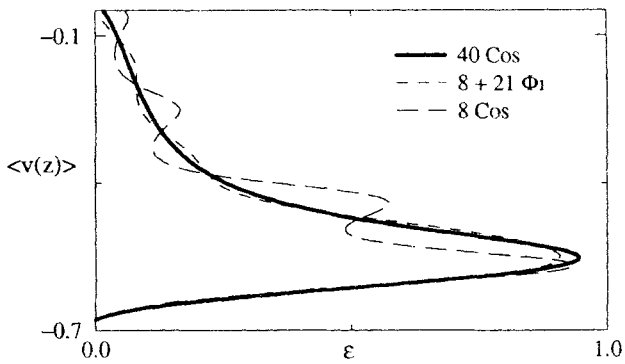


**Figure 4. Galerkin and nonlinear Galerkin methods.**

Steady-state bifurcation diagram in the vicinity of the saddle-node bifurcation computed through different "flat" (linear) Galerkin truncations and an approximate inertial form (based on the $\Phi_1$ AIM; see text).

$$\Phi_1 = -A^{-1}Q_pF(r_p+0)$$
$$\cdots \qquad (27)$$
$$\Phi_n = -A^{-1}Q_pF(r_p+\Phi_{n-1}).$$

(Note that the existence of the inverse of the operator $A$ restricted to the subspace of "slaved" modes is guaranteed. In our case, $A = diag(-k_i^2)$ is diagonal, which makes its inversion straightforward.) Another AIM approximation is motivated by integrating the $q$-part of the Galerkin approximation *for a short time step* $\tau$ (with initial condition $r_q = 0$) using an implicit Euler method (Foias et al., 1988a):

$$\Phi(r_p) = -\tau(I+\tau A)^{-1}Q_pF(r_p+0). \qquad (28)$$

In the following we use the $p+q$ notation for our AIM-based models to denote a $p$ equation model with a slaving relation for modes $p+1$ to $p+q$ (Figure 4 shows computations with an 8+21 AIF). The use of such nonlinear Galerkin methods has been computationally demonstrated to lead to increased accuracy for computed bifurcation diagrams, without increasing the size of the vectorfield (Jolly et al., 1990; Brown et al., 1991). This is demonstrated in our case through the overlaid bifurcation diagrams in Figure 4.

There have been attempts to extend the formalisms of both center manifolds (Cox and Roberts, 1991) and approximate inertial manifolds (Jones and Titi, 1994) for nonlinear PDEs with additional input ("spatiotemporal forcing"). In our case, we are interested in forcing described by the product of time-dependent amplitude(s) $u(t)$ and constant-shape actuator influence function(s) $q(z)$); the original evolution equation then becomes

$$dr/dt + Ar + F(r) + u(t)q(z) = 0, \qquad (29)$$

or, splitting it again formally in "slow" and "fast" dynamics $r_p$ and $r_q$,

$$\dot{r}_p + Ar_p + P_pF(r_p+r_q) + B_pu = 0 \qquad (30)$$

$$\dot{r}_q + Ar_q + Q_pF(r_p+r_q) + B_qu = 0, \qquad (31)$$

where $B_{p,q}$ denote projection of the actuator influence function $q(z)$ (the forcing term) onto $P_pH_n$ and $Q_pH_n$. Formally using the $\Phi$ maps (e.g., $\Phi_1$) employed for open-loop approximate inertial manifold construction leads then to $u$-dependent slaving relations such as

$$r_q = \Phi_1(r_p, u) = -A^{-1}[Q_pF(r_p+0) + B_qu], \qquad (32)$$

which yield the "forced" approximate inertial form

$$dr_p/dt + Ar_p + P_pF[r_p + \Phi_1(r_p, u)] + B_pu = 0. \qquad (33)$$

This is precisely the reduced model whose linearization around the desired set point will be used for construction of a (linear) stabilizing AIM-based controller.

### *Discretization with empirical orthogonal eigenfunctions (proper orthogonal decomposition)*

In the (semi-empirical) proper orthogonal decomposition (POD)-Galerkin method, the basis set for the spectral discretization of a DPS is obtained by statistical analysis of extensive spatiotemporal data obtained from the full system itself. An up-to-date review of the method can be found in a recent book by Holmes et al. (1997). Proposed in a 1956 report in the context of meteorology by Lorenz (Lorenz, 1956), the method was used as a means for identifying coherent structures in turbulent flows by Lumley (see book by Holmes et al. (1997) and references therein). Its use in the dynamical systems context was pioneered in the 1980s in Aubry et al. (1988) and the sequence of papers by Sirovich (e.g., Sirovich and Rodriguez, 1989). The basic steps leading to a low-dimensional dynamical system describing the DPS in question include:

- Forming a database ensemble of spatiotemporal data (obtained from integration of the full model).
- Extracting an empirical eigenfunction basis from the data.
- Generating a dynamical system describing temporal evolution of the modal coefficients of the solution expanded in these basis functions.

The first of these steps is by far the most crucial for the success of the venture: the ensemble is the starting point for forming the finite-dimensional subspace (a hyperplane) onto which the evolution PDE is later projected by the Galerkin procedure. All motions orthogonal to this hyperplane will be neglected, and the resulting error is assumed to be small in some sense. The necessity for a large simulational data set, the difficulty in obtaining it, and the lack of rigorous theoretical results concerning convergence properties underscore the empirical nature of the method; on the other hand, it has been rather successful in tackling problems beyond the conventional discretizations (see, for example, Deane et al., 1991, Adomaitis, 1997; Sahan et al., 1997; Aling et al., 1997).

The spatiotemporal data in the ensemble are stored in the "snapshot matrix" $SM \in R^{m\times n}$. The number of columns ($n$) corresponds to the number of snapshots (instants at which the state of the system has been captured), while the number of rows ($m$) is equal to the number of "pixels" (discretization points, coefficients of Fourier basis functions used in the simulations, etc.) This so-called "snapshot method" is appropriate when the relevant number of snapshots ($n$) is significantly smaller than the dimension of the discretization ($m$); if this is not case, an eigenanalysis of the two-point correlation matrix is used instead (Holmes et al., 1997).

Singular value decomposition (SVD) of the snapshot matrix represents it as a sum of rank-one matrices

$$SM = \sum_{i=1}^{n} \sigma_i t_i^T s_i \qquad (34)$$
$$\sigma_1 > \sigma_2 > \cdots > \sigma_n,$$

where $\sigma_i, t_i, s_i$ represent the singular values and vectors of the snapshot matrix $SM$.

A high degree of spatiotemporal coherence in the data ensemble will manifest itself in the almost zero magnitude of many of the singular values $\sigma_i$, and consequently, in the fact

that a relatively low-order ($p \ll n$) truncation of the preceding summation will provide a good approximation to *SM*. It is precisely the singular vectors $s_i$ retained in this low-order truncation that constitute the basis of the low-dimensional subspace used for spectral discretization of the original PDE (e.g., Eq. 29). In our implementation the basis functions were extracted from the database generated by time-integrations of a pseudospectral vector field. Thus, the spatial derivatives of the basis functions necessary in forming a KL-Galerkin vector field could be easily computed.

Making the ansatz

$$r(z,t) = \sum_{i=1}^{p} c_i(t) s_i(z) \tag{35}$$

for the solution, substituting it in the PDE, and demanding that the residual be orthogonal to the basis functions leads to the required low-dimensional dynamical system (here we are slightly abusing the notation $s_i(z)$; the $s_i$ are vectors whose elements come from spatial discretization, hence the dependence on the spatial variable $z$):

$$F(\dot{c}, c, u) = 0. \tag{36}$$

Notice that the parametric (e.g., $u$) dependence of the original DPS is *explicitly* retained in the low-order model. For simple forms of the nonlinearity (e.g., quadratic), the low-dimensional vectorfield can be constructed in explicit form (Deane et al., 1991; Bangia et al., 1997)—the numerical coefficients of the monomials arising due to the interaction of different modes are computed "off-line", in advance. For high-order and/or nonpolynomial nonlinearities, a pseudospectral discretization can be employed (Canuto et al., 1988; Kwasniok, 1997). The absence, however, of a numerical "fast POD transform" (analogous to the FFT for Fourier modes) makes the evaluation of the vectorfield and Jacobian for POD-based models rather expensive computationally (e.g., Aling et al., 1997).

Some practical comments about the method are in order. There are no *a priori* comprehensive rules for generation of the ensemble from which the empirical basis functions will be extracted. The data should be "fully representative" of (i.e., should span) the region of phase space in which studying temporal evolution or controlling the DPS is desirable. Since we are interested in good representation of the dynamics of the closed-loop system, the response of our dynamical system to possible actions of the available actuators should be somehow incorporated in the ensemble. Reported "common sense" ways of forming a potentially representative ensemble include combination of spatiotemporal motions at several values of operating parameters (Deane et al., 1991; Bangia et al., 1997), mixing transients from initial conditions distributed randomly around the relevant regions of phase space (Graham and Kevrekidis, 1996), and storing responses to perturbation of actuators from their nominal settings (Aling et al., 1996, 1997; Adomaitis, 1997; Park and Cho, 1996; Loffler and Marquardt, 1992).

For our example, the properties and capabilities of the POD-Galerkin method are illustrated in Figure 5. We formed our ensembles in the neighborhood of a nominal open-loop parameter value, combining transients at several parameter values with random forcing of the amplitudes of the actuators; data were sampled after the very fast part of the dynamics decayed to the neighborhood of the system attractor. In our implementation this procedure was performed separately for $v(z)$ and $w(z)$ fields in the FitzHugh-Nagumo PDE. Simulations of the reaction-diffusion system yielded two ensembles (for $v(z)$ and $w(z)$ fields) that were later SV-decomposed to form separate basis sets ($\phi_i$ and $\psi_i$, respectively) for spectral discretization. An alternative implementation could have the "stacked" profiles ($v(z)$; $w(z)$) in the ensemble, taking into account in this way the correlation between the two variables. The spatially localized nature of the resulting empirical eigenfunctions is demonstrated in Figure 5a. The first four eigenfunctions contain $> 99\%$ of the energy (in the least-squares sense) of the ensemble. They satisfy the boundary conditions by construction and are tailored to the problem: capturing dynamics in the vicinity of the sharp frontlike

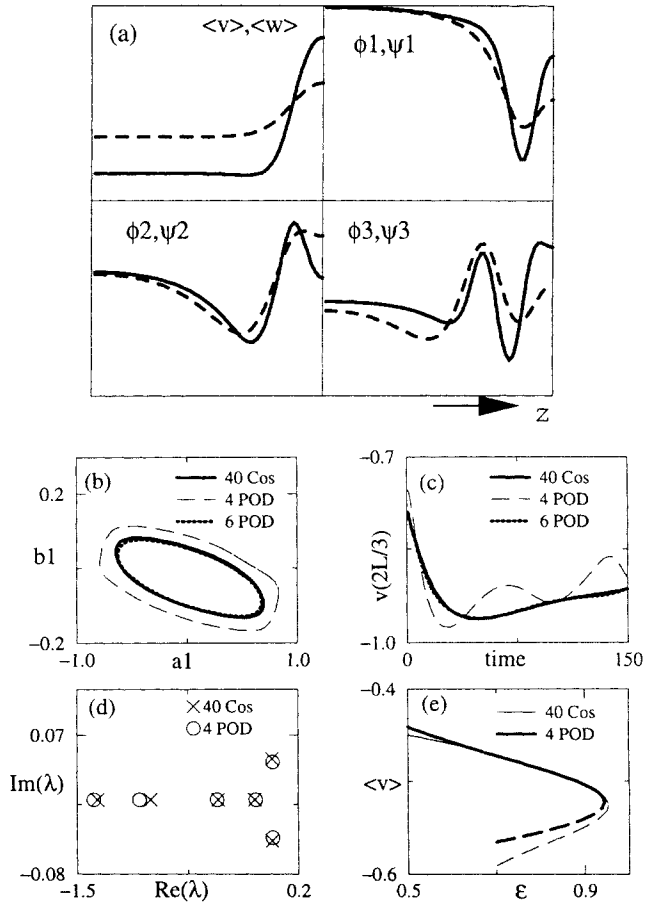


**Figure 5. POD-Galerkin methods.**

(a) Leading empirical eigenfunctions obtained near the saddle-node bifurcation at $\epsilon \in (0.7\text{–}0.9)$. Solid/dashed line-$v/w$ basis functions, (b) comparison of attractors at $\epsilon = 0.015$ predicted by conventional and POD Galerkin vectorfields. (c) Short-time prediction capabilities of POD-Galerkin methods. Starting with a given profile, the value of $v$ at $z = 2L/3$ is plotted from transients of conventional and POD-Galerkin vectorfields ($\epsilon = 0.015$). (d) Comparison of the leading part of the spectra of the linearization of the unstable steady state at $\epsilon = 0.015$ computed through conventional and POD-Galerkin models. (e) Alternative bifurcation diagrams of the front-type solutions near the saddle-node bifurcation.

steady state. The validity of the low-dimensional dynamical systems generated by Galerkin procedure based on these eigenfunctions can be tested by considering the ability of the resulting truncation to accurately approximate the location of the steady state and its linearization as well as by its short-term tracking capabilities. An illustration of the former is presented in Figure 5b, where attractors computed with high-order cosine spectral discretization are compared to those computed with POD-based vectorfields. Projection of our spatiotemporal limit cycle on the first two empirical eigenfunctions computed with POD-Galerkin based on six modes is very close to the converged attractor computed with the full model. The same vectorfields are successful in short-term tracking of off-attractor dynamics. Note that, while the long-term prediction properties of a four-mode (eight-equation) vector field eventually deteriorate, the short-term prediction quality can be quite reasonable for time scales of the order of one-tenth to one-sixth of the natural period of the oscillation, Figure 5c. The ability of the vector fields to predict the location and spatial structure of a steady or oscillatory state (unstable stationary front for parameters in Figure 5d) is combined with their ability to approximate closely the leading part of the corresponding spectra (eigenvalues, Floquet multipliers). The explicit parametric dependence of the generated vectorfields is crucial for the computation of bifurcation diagrams for the problem solutions and for controller design. This is illustrated in the alternative (62-dimensional Fourier discretization vs. 8-dimensional POD-based) computation of the open-loop bifurcation diagram in Figure 5(e).

## Linear Feedback Control

### *Closed-loop system*

In this section we demonstrate the design and performance of controllers based on reduced-order vector fields. More specifically, the controllers are based on the linearization of the low-order nonlinear vectorfields, obtained through the methods described in the previous section, around the set point (an unstable steady state at a nominal parameter value). Steady-state computations, linearization, and controller design (here using the Control Toolbox of *MATLAB*) take advantage of the explicit parametric dependence of the reduced-order models. Pole placement (Kautsky et al., 1985) and optimal control (LQR) methods (Bryson and Ho, 1975) were used for controller design (`place(A, B, p)` and `lqr(A, B, q, r)` *MATLAB* routines, respectively). The matrix of gains ($K$) was then incorporated in the full nonlinear vectorfield describing the evolution of the reaction-diffusion system (31 Cosine Galerkin truncation resulting in a 62-dimensional vectorfield). For our particular example, the implementation of this full closed-loop vectorfield is outlined briefly below.

The no-flux boundary conditions give rise to a cosine expansion of both fields:

$$v(z,t) = \sum_{i=1}^{n} a_i(t)\cos\pi(i-1)z/L, \tag{37a}$$

$$w(z,t) = \sum_{i=1}^{n} b_i(t)\cos\pi(i-1)z/L. \tag{37b}$$

The $n$-mode Galerkin truncation takes the form

$$\dot{a}_i = -(i-1)^2(\pi/L)^2 a_i + \hat{f}_i(a,b) + \sum_{j=1}^{s} u_j \hat{q}_{ij} \tag{38}$$

$$\dot{b}_i = -\delta(i-1)^2(\pi/L)^2 b_i + \hat{g}_i(a,b), \tag{39}$$

where

$(\vec{a};\vec{b}) \equiv \vec{x} \in R^{2n}$, $n$ = the number of modes in the full Galerkin models (the factor two comes from the two PDEs in the FitzHugh-Nagumo system);

$\vec{u} \in R^s$, $s$ = the number of actuators;

$\vec{e} = \vec{y} - \vec{y}^0 \in R^{2m}$ = the projection of the error on the low-dimensional subspace in which the solution is controlled; $2m (m \ll n)$ is the order of the reduced linearized model $\dot{\vec{e}} = A\vec{e} + B\vec{u}$ used for controller design;

$$B_{2n\times s}: B = \begin{pmatrix} Q_{n\times s} \\ 0_{n\times s} \end{pmatrix},$$

where

$Q_{n\times s}$: $Q_{ij} = \langle q_j(z), \cos(i-1)z/\mathrm{L}\rangle$ = is the $i$th Fourier component of the $j$th actuator influence functions;

$\hat{g}_i(a,\mathrm{b})$ and $\hat{f}_i(a,b)$ = are components of the Cosine transform of the kinetic terms in the PDE (which are, in general, nonlinear).

For linear feedback the vector of actuator amplitudes will be given by

$$\vec{u} = -K\vec{e} = -K(\vec{y} - \vec{y}_0) = -K(P\vec{x} - \vec{y}_0). \tag{40}$$

Here $K_{s\times 2m}$ is a matrix of gains; $\vec{y} \in \boldsymbol{R}^{2m}$ is the state projected on the subspace of the reduced model. The full state ($\vec{x} \in R^{2n}$) is projected on a selected set of modes (Fourier modes, POD modes, etc.) through the orthogonal projector $P$:

$$P_{2m\times 2n} = \begin{pmatrix} M & 0_{m\times n} \\ 0_{m\times n} & L \end{pmatrix}. \tag{41}$$

When the linear regulator is designed to control the first $m$ Fourier coefficients of the "full" model, $M$ and $L$ are

$$M = L = (I_{m\times m} \mid 0_{m\times(n-m)}). \tag{42}$$

When the error is controlled in the space of modal coefficients on some other set of modes (orthogonalized set of eigenvectors for some steady state, POD modes), these matrices are

$$M_{ij} = \langle \phi_i^v(z), \cos(j-1)z/L\rangle \quad L_{ij} = \langle \psi_i^w(z), \cos(j-1)z/L\rangle, \tag{43}$$

where $\phi_i^v(z)$ ($\psi_i^w(z)$) are the $i$th($j$th) POD mode for the $v(w)$ component of the state. The closed-loop nonlinear system is then

$$\dot{\vec{x}} = \vec{F}(\vec{x}) + B\vec{u} = \vec{F}(\vec{x}) - BK(P\vec{x} - y^0). \tag{44}$$

Here $y^0$ is the projection of the set point (the steady state of

the full Galerkin model) on the subspace of controlled modes; thus closing the loop perturbs only the linearization of the system around the set point, and not the set point itself. This is a small but important point that we will revisit below: the fact that the steady states (at the nominal parameter value) of the reduced models are *approximations* of the true set point.

While success for the linear stabilization problem is easily tested by linearization of the closed-loop steady state, additional effort is required to obtain information about the global phase space structure of the closed-loop system (e.g., the possibility of competing attractors and some estimate of their basin boundaries). We chose to obtain such global information through a homotopy procedure that allows us to correlate the open-loop (presumably known) global phase-space structure to that of the closed loop. We performed a continuation of the open-loop attractors as illustrated in Figure 6. In an article by Chang and Chen (1984) such a continuation was performed using the controller gains as the homotopy parameters. In the case of MIMO feedback control, a single parameter can be used to link the open loop ($\alpha = 0$) with the closed loop ($\alpha = 1$) dynamics. We will use the term "correlation diagram" to describe the bifurcation diagrams in $\alpha$ (Figure 6).

We now proceed to the discussion of our two computational examples.

### *Numerical examples*

*Stabilization of a Saddle.* We used a single actuator with influence function shown in Figure 7c to stabilize an unstable, saddle-type front solution at $\epsilon = 0.8$, close to the saddle-node bifurcation ($\epsilon \approx 0.9445$) in Figure 2c. The set point as well as a blowup of the relevant portion of the steady-state bifurcation diagram are shown in Figure 7a and 7b.

Earlier we compared some of the open-loop bifurcation diagrams obtained with various reduced models; Table 1 illustrates the leading part of the spectrum of the saddle steady states of these models. These were computed at the "set point" parameter value ($\epsilon = 0.8$); the accuracy of the particular spectrum predicted by the 8-D dynamical system resulting from the four-mode POD-Galerkin truncation is remarkable.

After verifying that the linear systems resulting from the linearized low-order vector fields were stabilizable, single-input pole-placement controllers were designed for the set points. The critical eigenvalue in each case was shifted to $-0.3$ by the design procedure, while the rest of the closed-loop spectrum was left intact. When the resulting controllers were implemented on the full 62-dimensional vectorfield the table of (now stable node) closed-loop spectra was obtained (Table 2).

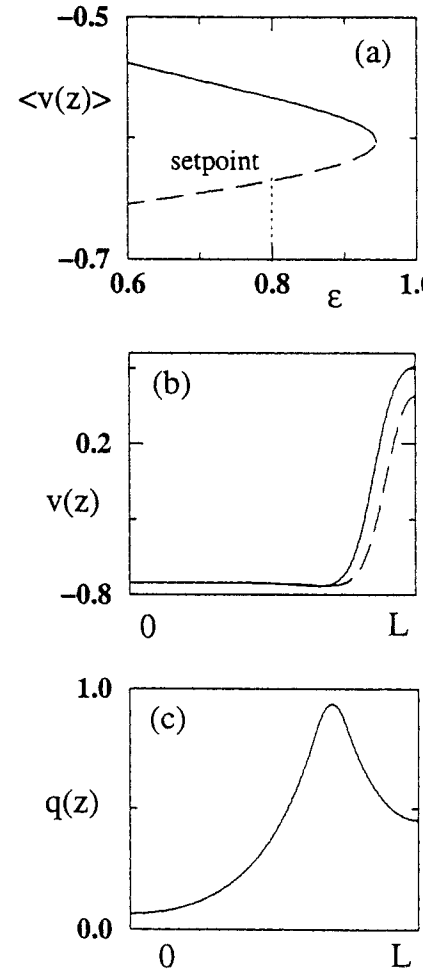


**Figure 7. Stabilization of an unstable (saddle) front steady state close to the saddle-node bifucation.**

(a) Steady-state bifurcation diagram, showing the set point (at $\epsilon = 0.8$). (b) Spatial profiles corresponding to the saddle (dashed line) and node (full line) at that value of $\epsilon$. (c) Spatial profile of the actuator influence function.

We see that all controllers are, in principle, successful in stabilizing the open-loop unstable setpoint; the shift of the critical eigenvalue is not, however, equally accurate in the various cases.

The "fate" of the various open-loop attractors after feedback is illustrated in the correlation diagrams of Figure 8. These were computed for the linear stabilizing controllers based on (a) a four-mode POD and (b) an $8+21$ $\Phi_1$ AIM reduced model, respectively. The open-loop ($\alpha = 0$) attrac-

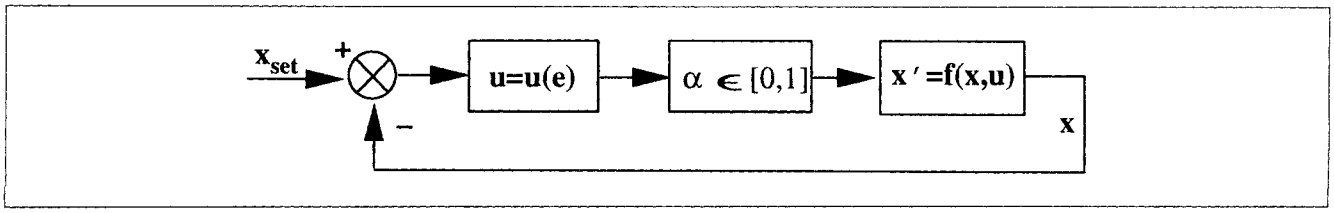


**Figure 6. Single-parameter homotopy used to correlate the open loop with the closed-loop dynamics.**

**Table 1. Open-Loop Leading Eigenvalues (Saddle)**

| Model for Controller Design | $\lambda_1$ | $\lambda_2$ | $\lambda_3$ |
|---|---|---|---|
| 31 cos | 0.1266 | $-0.7385$ | $-1.1014 \pm 0.7190\,i$ |
| 11 cos | 0.0908 | $-0.7522$ | $-1.1017 \pm 0.7191\,i$ |
| $\Phi_1$ : 6 + 15 | 0.1952 | $-1.1049 \pm 0.7178\,i$ | $-1.2430$ |
| $\Phi_1$ : 8 + 21 | 0.1065 | $-0.7905$ | $-1.1022 \pm 0.7188\,i$ |
| 4 POD | 0.0588 | $-1.0118$ | $-1.2074 \pm 0.6676\,i$ |

tors are shifted, and in both cases the (far away in phase space) branch of extinguished uniform steady states disappears through saddle-node bifurcations for $\alpha < 1$. The same effect is observed for the branch of "ignited" uniform steady states for the case of the AIM-based controller, while for the POD-based controller the branch of ignited steady states persists up to the closed loop ($\alpha = 1$).

It is important to notice that the sought-for exchange of stability of the (initially saddle) set point occurs through a *transcritical* bifurcation for $\alpha < 1$. Normal-form analysis shows that this is generic for (linear) stabilization of a saddle close to a saddle-node bifurcation. It is well known (Gukenheimer and Holmes, 1983) that transcritical bifurcations (imposed here by the nature of the closed loop, which keeps the steady state independent of $\alpha$) are structurally unstable, and will generically break under the effect of perturbations.

A natural source for a perturbation that will break this transcritical bifurcation is the modeling error introduced by the reduction process: in particular, the mismatch between the full and reduced model steady states. If the set point supplied to the closed-loop system is chosen to be the saddle solution *of the low-dimensional model itself*, not only the linearization, but also the steady state of the closed-loop system will be slightly affected. For both controllers (4 POD- and 8 + 21 AIM-based) the predicted saddle solution is close to the converged one (Figures 9a and 9b—note the scale on both figures, and the way the error is distributed across the domain). The closed-loop stability is affected in two markedly different ways. For the AIM-based controller the breakup of the transcritical bifurcation shows that the closed-loop stable steady state "comes from" (is a smooth continuation in $\alpha$ of) the open-loop node. For the 4 POD-based controller, however, an alternative breakup of the transcritical bifurcation leads to two saddle nodes in the bifurcation diagram with respect to $\alpha$, one shown in the figure, and one further to the right (not shown). As a result of this breakup, no nearby stable steady state exists for the closed-loop system (for $\alpha \approx 1$).

The implications of these changes in the steady-state structure are explored through transient simulations of the closed-loop system. The AIM-based controller successfully drives the system to a steady state that is rather close to the

**Table 2. Closed-Loop Leading Eigenvalues (Stabilized Node)**

| Model for Controller Design | $\lambda_1$ | $\lambda_2$ | $\lambda_3$ |
|---|---|---|---|
| 31 cos | $-0.3000$ | $-0.7385$ | $-1.1014 \pm 0.7190\,i$ |
| 11 cos | $-0.2355$ | $-0.7618$ | $-1.1019 \pm 0.7193\,i$ |
| $\Phi_1$ : 6 + 15 | $-0.3384$ | $-0.7421$ | $-1.1017 \pm 0.7522\,i$ |
| $\Phi_1$ : 8 + 21 | $-0.2558$ | $-0.7287$ | $-1.1034 \pm 0.7191\,i$ |
| 4 POD | $-0.0822$ | $-0.7469$ | $-1.0845 \pm 0.7132\,i$ |

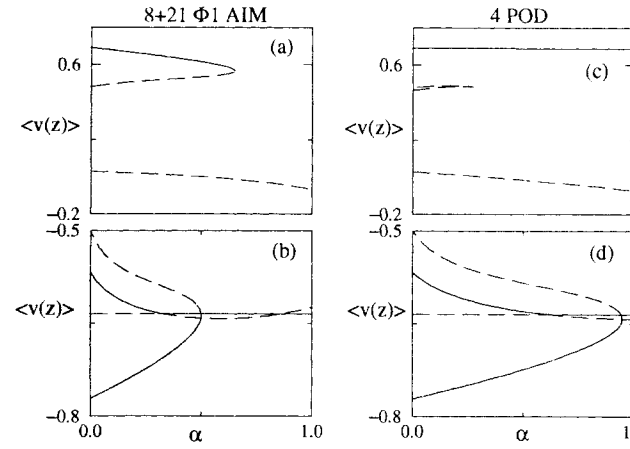


**Figure 8. Effect of the linear controller on the open-loop dynamics.**

"Correlation diagrams" computed for a 62-dimensional vectorfield, starting at open-loop ($\alpha = 0$) and terminating at $\alpha = 1$ with closed-loop vectorfields, stabilized by controllers based on 16-dimensional (AIM-based, left) and 8-dimensional (POD-based, right). *Y*-axis corresponds to the zeroth Fourier mode of $v(z)$. The diagrams show the fate of the open-loop steady states coexisting with the set point as the loop closes. (The vertical axes in both figures are broken).

set point (both in the open- and closed-loop systems). The eventual convergence to a stationary front solution can be achieved from different initial conditions (for example, starting close to the open-loop node, Figures 10a, 10d, 10g, and the open-loop extinguished steady state, Figures 10a, 10b, 10e, 10h). This successful performance (even in the face of perturbation due to the modeling error of the set point) is contrasted with the simulations for the full system with the four POD-based controller. Closing the loop, and starting very close to the set point (as predicted by the low-dimensional model), the controller leads to unstable response; since modeling error has destroyed all steady states in the neighborhood, the system is driven away from the set point, ending eventually close to what, for the open loop, was the extinguished uniform steady state.

*Stabilization of a Focus.* For this example we chose multivariable (three actuators) controllers designed to stabilize the unstable front solution at $\epsilon = 0.015$ (Figure 11). Table 3 summarizes the leading spectra of the open-loop, unstable foci computed through various reduced-order models, while Table 4 shows the relative success in closed-loop pole placement (for the full model) of controllers designed to place the real part of the open-loop unstable eigenvalue pair of the reduced models at $-0.3$.

We now compare results for two distinct linearly stabilizing controller designs (MIMO pole placement and LQR) based on an 8-dimensional POD-mode-based vector field. The linear optimal feedback controller was designed to minimize the cost functional

$$J = \int_0^\infty (y^T Q y + u^T R u)\, dt \tag{45}$$

with weighting matrices (Bryson and Ho, 1975):

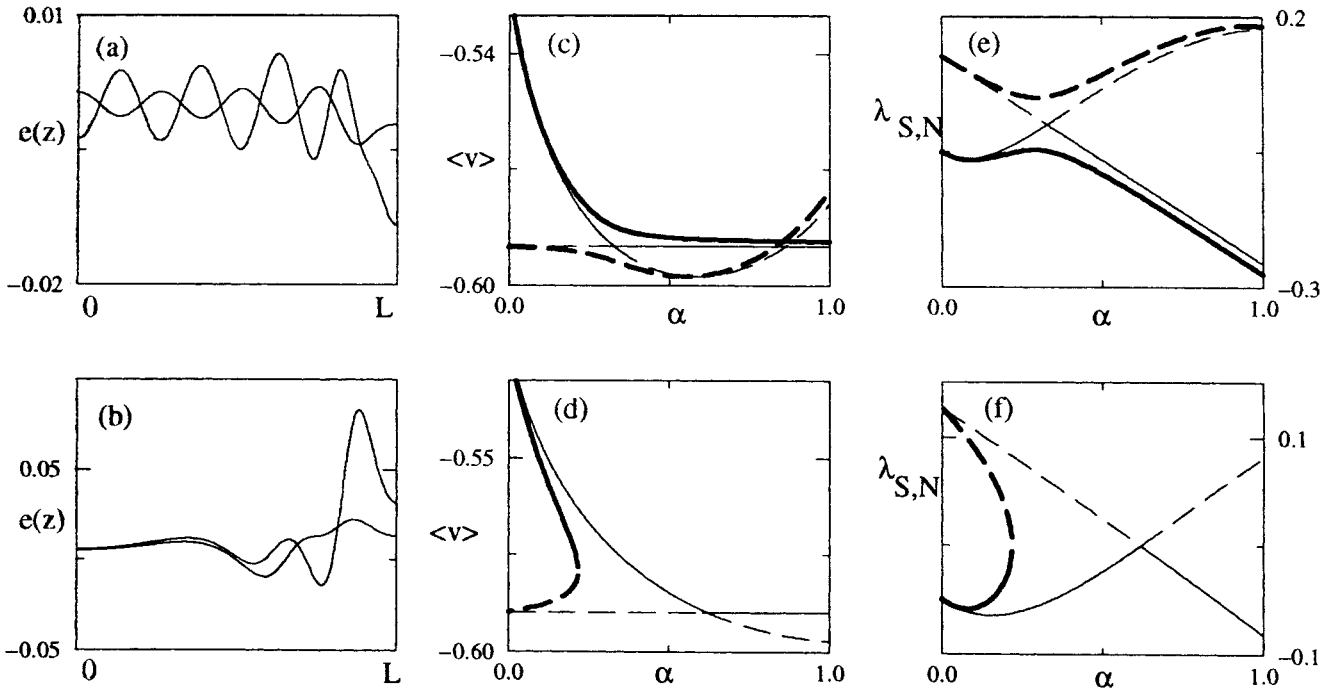


**Figure 9. Steady state of reduced-order model as the set point for the full closed loop.**

Spatial form of errors in the set point computed through an $8+21\Phi_1$ AIM (a) and a 4-mode POD Galerkin vectorfield (b). Correlation diagrams relating the steady states (c,d) and eigenvalues (e,f) of the open-loop system ($\alpha = 0$) to those of the closed-loop system ($\alpha = 1$). The open-loop set point (saddle) has $\langle v \rangle = -0.5853$, while the open-loop node has $\langle v \rangle = -0.5167$; stable (unstable) branches and eigenvalues are indicated with solid (broken) lines, respectively. Top (bottom): AIM (POD) -based controllers.

$$R = \text{diag}(1, 1, 1), \qquad Q = \text{diag}(\beta_1, \beta_2, \ldots, \beta_{2m}). \quad (46)$$

The $\beta_i$ were chosen to be the maximum absolute values of the variables along the limit cycle surrounding the open-loop unstable steady state. The $\beta_i$ values ranged from 0.9 to 0.03 for the $v$ field, and from 0.14 to 0.001 for the $w$ field (decreasing for higher modes).

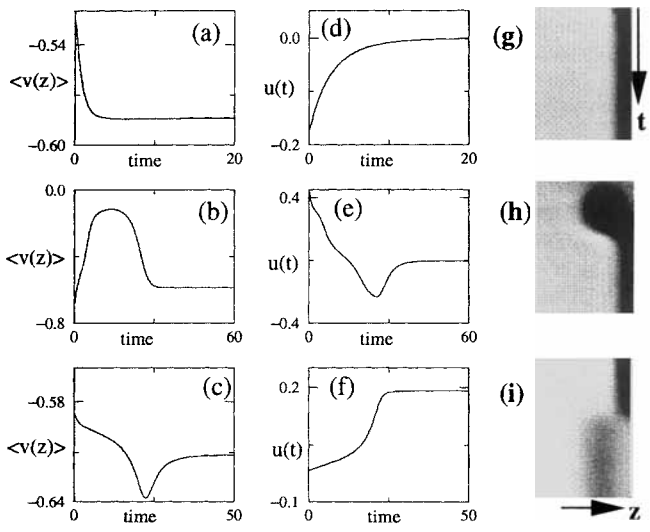


**Figure 10. Transient simulations of closed-loop systems with pole-placement controllers based on reduced-order vector fields.**

(a,b,c) Temporal evolution of the zeroth mode of $v(z)$. (d,e,f) Control histories, and (g,h,i) space–time plots for the evolution (in grayscale) of $v(z,t)$. (a,b) AIM-based vector field. Directing the system to the set point from an initial condition chosen at the open-loop node front-type steady state (a) and at the open-loop uniform extinguished steady state (b). (c) The runaway transient resulting from using the steady state of the 4-mode POD Galerkin vector field as a setpoint.

Both controllers were tested through simulations for the full closed-loop system. Starting on the open-loop limit cycle, Figure 12a and 12c present an example of stabilization: swinging oscillations of a front are suppressed, the front is driven to the set point prescribed position, and the control action goes to zero. Figure 12d is intended to demonstrate the markedly different basins of attraction of the (locally stable) full-model closed-loop steady state for the two different controller designs: the LQR controller successfully drives the front to the (locally stabilized) set point from every initial condition along what used to be the open-loop limit cycle. In contrast, stabilization is achieved for a markedly smaller subset of these initial conditions by the pole-placement controller. This is perhaps not surprising, since the latter does not penalize the excessive control action that might result in temporal runaway behavior. Finally Figure 12e presents a comparison of open- and closed-loop (LQR design) responses to "noise," small-amplitude periodic disturbances in one of the system parameters ($\epsilon$). We see that the controller keeps the closed loop in a small neighborhood of the set point, while the open-loop response is unstable.

## Summary and Discussion

The purpose of this article was to demonstrate that systematic methods of model reduction (whether *a priori*, such as approximate inertial manifold-based, or semiempirical, such as POD-based) can be successfully used to design controllers

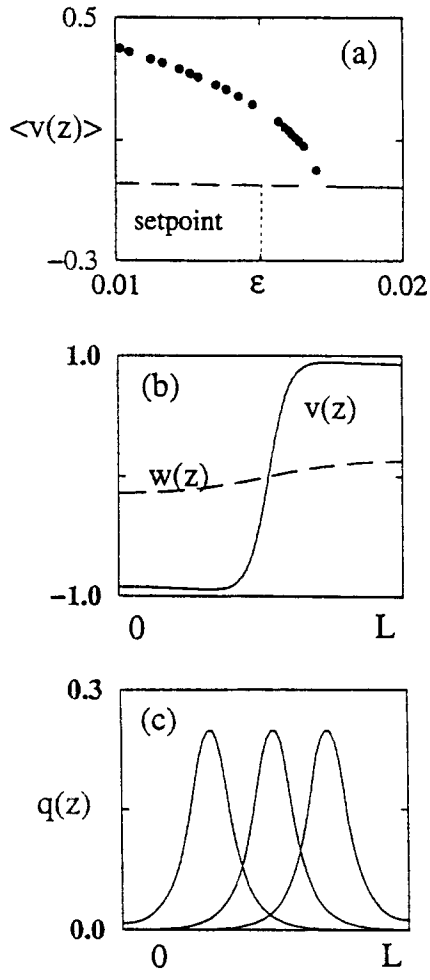


**Figure 11. Stabilization of an unstable front with a single unstable complex conjugate pair.**

(a) Open-loop steady-state bifurcation diagram in the neighborhood of the Hopf bifurcations showing the set point at $\epsilon = 0.015$. (b) Spatial profile of the two variables for the open-loop unstable front (set point) for the closed loop). (c) Spatial form of the three actuator influence functions.

for nonlinear distributed parameter systems. Model-reduction procedures (open- and closed-loop) in the presence of sharply varying solutions and actuator-influenced functions constituted the focus of this effort. In the absence of disturbances the controller design was relatively simple (pole-placement and LQR), and, more importantly, we assumed that the full state was available for feedback, and did not have to consider observers.

We also made an effort to relate the open-loop nonlinear dynamics (e.g., multiple attractors) with the closed-loop dynamics through correlation diagrams. Systematic steps can be taken to incorporate issues such as nonlinear controller design, deterministic disturbances, observer design, and actuator/sensor dynamics. In particular, we expect a significant increase in the performance of the closed-loop systems (e.g., the basins of attraction of the closed-loop set points) when nonlinear controllers (e.g., feedback linearization or model predictive control) are used: these will take true advantage of the fully nonlinear reduced models we construct, something we did not exploit here. When more is known about the global phase-space structure of the open-loop system (such as the global heteroclinic connections, Coller et al., 1994), this knowledge may be exploited in designing nonlinear controllers for the particular problem. Here we concentrated on stabilization; reduced vectorfields can, of course, also be used for tracking purposes (see Aling et al., 1995, for an example of the exploitation of POD-based models).

Depending on the approach used for model reduction in a closed-loop context, a variety of conceptual and practical problems arise: for the POD-based approach the most important issue is the generation of a "representative" data set, so that the resulting basis functions span the closed-loop dynamics. While this cannot be guaranteed *a priori*, one can use the available actuators systematically, so that the relevant region of the state space (around the set point, or, more generally, a nominal trajectory) is sampled as uniformly as possible. For AIM-based methods, theoretical work is needed to establish the relation of the (presumably known) open-loop low-dimensional behavior with the particular AIMs that result from particular choices of controllers (and actuators). Estimates of the dimension of the closed-loop IMs (how many degrees of freedom need to be kept) as well as the error between the full closed-loop dynamics and the reduced closed-loop vector fields (AIFs with feedback) are just starting to appear.

Everything we discussed here is based on the availability of the "full model": a code, based on the large, converged, accurate "conventional" discretization of a first-principles model of the process (a vectorfield, and, possibly, its Jacobian). This also is true for the systematic theoretical work on linear DPS. Reducing this vectorfield, while conceptually straightforward,

**Table 4. Closed-Loop Leading Eigenvalues (Stabilized Focus)**

| Model for Controller Design | $\lambda_1$ | $\lambda_2$ | $\lambda_3$ | $\lambda_4$ |
|---|---|---|---|---|
| 8 cos | $-0.1118 \pm 0.0245i$ | $-0.1395$ | $-0.4167$ | $-0.9422$ |
| $\Phi_1 : 8+21$ | $-0.1170 \pm 0.0094i$ | $-0.1408$ | $-0.4192$ | $-0.9383$ |
| 7 POD | $-0.0456$ | $0.1387$ | $-0.4214$ | $-0.7063$ |
| 4 POD | $-0.0469$ | $0.1374$ | $-0.4208$ | $-0.6811$ |
| 4 POD(LQR) | $-0.0514 \pm 0.0492i$ | $-0.1386$ | $-0.4210$ | $-0.9411$ |

**Table 3. Open-Loop Leading Eigenvalues (Unstable Focus)**

| Model for Controller Design | $\lambda_1$ | $\lambda_2$ | $\lambda_3$ | $\lambda_4$ |
|---|---|---|---|---|
| 31 cos | $0.0011 \pm 0.0450i$ | $-0.1386$ | $-0.4209$ | $-0.9411$ |
| 4 cos | $-0.0777$ | $-0.1395$ | $-0.1847$ | $-0.3864$ |
| 8 cos | $-0.0247 \pm 0.0620i$ | $-0.1387$ | $-0.4171$ | $-0.9401$ |
| $\Phi_1 : 8+21$ | $-0.0056 \pm 0.0504i$ | $-0.1383$ | $-0.4206$ | $-0.9391$ |
| 4 POD | $0.0032 \pm 0.0427i$ | $-0.1293$ | $-0.4617$ | $-1.3193 \pm 0.0676\,i$ |
| 7 POD | $0.0021 \pm 0.0442i$ | $-0.1385$ | $-0.4261$ | $-0.9603$ |

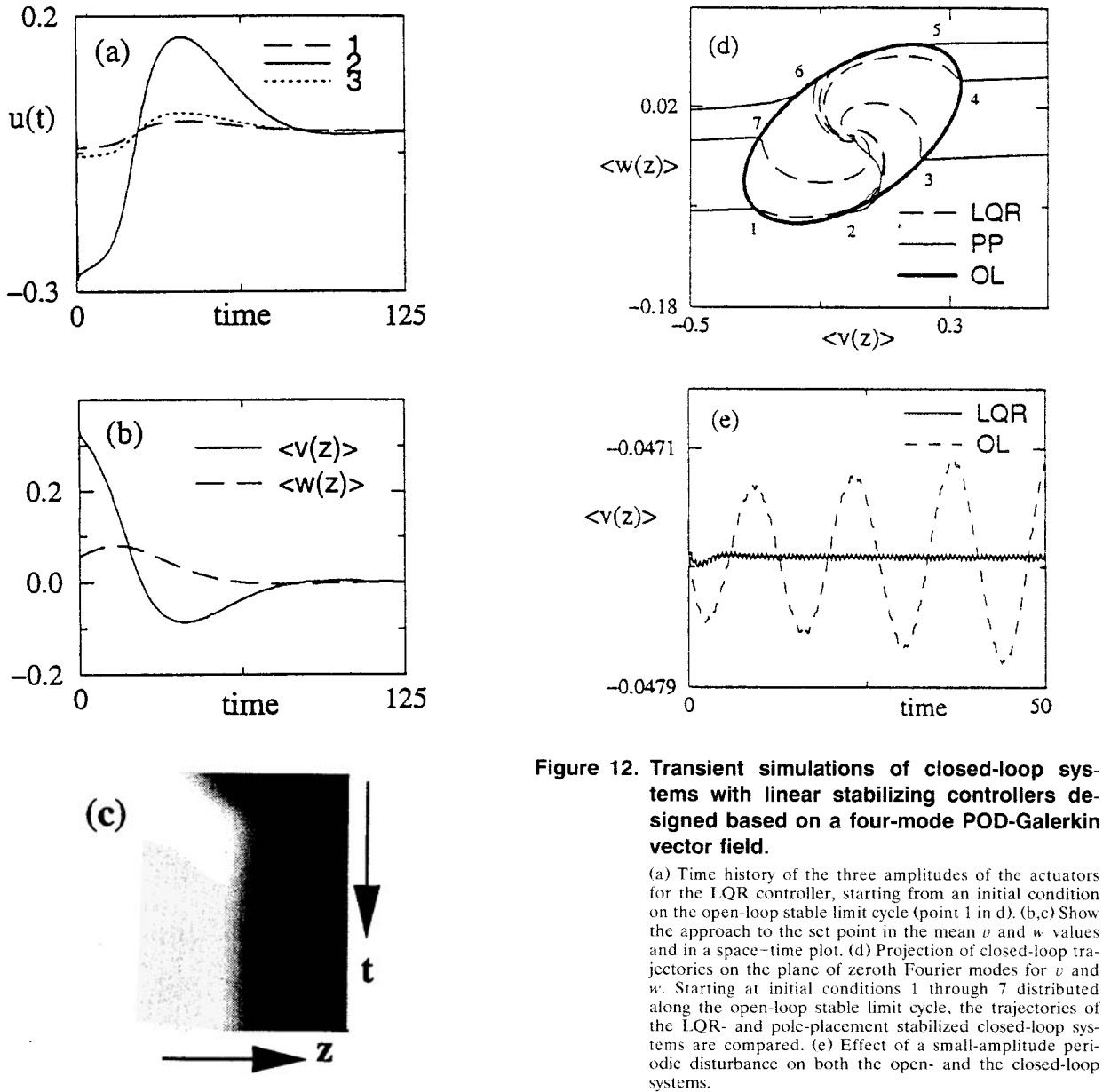


**Figure 12. Transient simulations of closed-loop systems with linear stabilizing controllers designed based on a four-mode POD-Galerkin vector field.**

(a) Time history of the three amplitudes of the actuators for the LQR controller, starting from an initial condition on the open-loop stable limit cycle (point 1 in d). (b,c) Show the approach to the set point in the mean $v$ and $w$ values and in a space–time plot. (d) Projection of closed-loop trajectories on the plane of zeroth Fourier modes for $v$ and $w$. Starting at initial conditions 1 through 7 distributed along the open-loop stable limit cycle, the trajectories of the LQR- and pole-placement stabilized closed-loop systems are compared. (e) Effect of a small-amplitude periodic disturbance on both the open- and the closed-loop systems.

gives rise to a different class of scientific computing problem. Evaluating the righthand side of the nonlinear POD-based reduced vectorfield is computationally very costly for nonlinearities higher than quadratic (or nonpolynomial, such as the Arrhenius temperature dependence). The memory required for storing the monomial coefficients of this righthand side explodes with the number of modes kept, while "fast-POD transforms" for a pseudospectral evaluation have not yet been developed. Conversely, the righthand sides of AIM-based reductions and especially their linearizations (which are important for stability analysis and controller design) become immensely complex (see, for example, Russel et al., 1993). As a result, a twenty-equation vector field, even though much better conditioned than the full model, may require a significant fraction of the time required to integrate the full model (up to 20–50% sometimes; e.g., Aling et al., 1997). Systematic approaches to speeding up the evaluation of these complicated righthand sides and derivatives would greatly enhance the appeal and applicability of these reduction methods.

We conclude with two practical comments. For stabilization problems and finite disturbances, one might expect that the closed-loop system will be "confined" to a finite region of state and parameter space in the neighborhood of the set point. POD-based models are particularly suited for efficient dimensionality reduction in such situations. The POD-based subroutine for the (costly) evaluation of the reduced vectorfield righthand sides (which includes explicit dependence on parameters and actuators) can be used off-line to train a black-box fit of this evaluation; such a fitted model is immensely faster to evaluate in real time. Finally, while tradi-

tional ("linear Galerkin") POD methods simply truncate to obtain a reduced model, it makes sense to combine separation of time scales with a good hierarchical basis for further model reduction: slave the "higher" POD-mode dynamics to the "lower" ones. This "two-tier" reduction may affect the criteria for selecting the POD-mode hierarchy (see, for example, Sirovich et al., 1990, and Aling et al., 1997, for an application).

## Acknowledgments

This research was partially supported through the National Science Foundation and ARPA/ONR grants. Part of the work was performed when one of the authors was at the ICEHT-FORTH (Patras, Greece) supported by a 94-PENED Grant. We are grateful to Professor Edriss S. Titi for helpful discussions and assistance.

## Literature Cited

Adomaitis, R. A., "An Orthogonal Collocation Technique for Rapid Thermal Processing System Discretization," *AIChE J.*, in press (1997).

Ajinkaya, M. B., M. Kohne, H. F. Mader, and W. H. Ray, "The Experimental Implementation of a Distributed Parameter Filter," *Automatica*, **11**, 571 (1975).

Aling, H., J. L. Ebert, A. Emami-Naeini, and R. L. Kosut, "Application of Nonlinear Model Reduction to Rapid Thermal Processing(RTP) Reactors," *Proc. Int. Rapid Thermal Processing Conf.*, R.B. Fair and B. Lojej, eds., Amsterdam, p. 356 (1996).

Aling, H., S. Banerjee, A. K. Bangia, V. Cole, J. L. Ebert, A. Emami-Naeini, K. F. Jensen, I. G. Kevrekidis, and S. Shvartsman, "Nonlinear Model Reduction for Simulation and Control of Rapid Thermal Processing," *Proc. Amer. Control Conf.*, Albuquerque, NM, 2233 (June 1997).

Aling, H., J. Abedor, J. L. Ebert, A. Emami-Naeini, and R. L. Kosut, "Application of Feedback Linearization to Models of Rapid Thermal Processing (RTP) Reactors," *RTP*, p. 356 (1995).

Ammi, A., and M. Marion, "Nonlinear Galerkin Methods and Mixed Finite Elements: Two-Grid Algorithms for the Navier-Stokes Equations," *Numer. Math.*, **68**, 189 (1994).

Aubry, N., P. Holmes, J. L. Lumley, and E. Stone, "The Dynamics of Coherent Structures in the Wall Region of a Turbulent Boundary Layer," *J. Fluid Mech.*, **192**, 115 (1988).

Badgewell, T. A., T. Breedijk, S. G. Bushman, S. W. Butler, S. Chatterjee, T. F. Edgar, A. J. Torpac, and I. Trachtenberg, "Modeling and Control of Microelectronics Materials Processing—Review," *Comput. Chem. Eng.*, **19**, 1 (1994).

Badmus, O. O., S. Chowdhury, and C. N. Nett, "Nonlinear Control of Surge in Axial Compression Systems," *Automatica*, **32**(1), 59 (1996).

Balas, M. J., "Feedback Control of Linear Diffusion Processes," *Int. J. Control*, **29**(3), 523 (1979).

Balas, M. J., "Reduced-Order Feedback Control of Distributed Parameter Systems via Singular-Perturbation Methods," *JMMA*, **87**, 281 (1982a).

Balas, M. J., "Toward a more Practical Control Theory for Distributed Parameter Systems," *Control Dyn. Syst.*, 361 (1982b).

Balas, M. J., "The Galerkin Method and Feedback Control of Linear Distributed Parameter Systems," *JMAA*, **91**, 526 (1983).

Balas, M. J., "Nonlinear Finite-Dimensional Control of a Class of Nonlinear Distributed Parameter Systems Using Residual-Mode Filters: A Proof of Local Exponential Stability," *JMAA*, **162**, 63 (1991).

Bangia, A. K., P. F. Batcho, I. G. Kevrekidis, and G. Em. Karniadakis, "Unsteady 2-D Flows in Complex Geometries: Comparative Bifurcation Studies with Global Eigenfunction Expansions," *SIAM J. Sci. Comput.*, **18**(3), 775 (1997).

Banks, H. T., R. C. Smith, D. E. Brown, R. J. Silcox, and V. L. Metcalf, "Experimental Confirmation of a PDE-Based Approach to Design of Feedback Controls," *SIAM J. Control. Optim.*, **35**(4), 1263 (1997).

Bansenauer, B. T., and M. J. Balas, "Reduced Order Model Based Control of the Flexible Articulated-Truss Space Crane," *Guid. Control. Dyn.*, **18**(1), 135 (1995).

Batcho, P. F., and G. E. Karniadakis, "Generalized Stokes Eigenfunctions: A New Trial Basis Function for the Solutions of Incompressible Navier-Stokes Equations," *J. Comput. Phys.*, **115**, 121 (1994).

Bequette, B. W., "Nonlinear Control of Chemical Processes: A Review," *Ind. Eng. Chem. Res.*, **30**, 1391 (1991).

Boley, D. L., "Krylov Space Methods on State-Space Control Models," *Circ. Syst. Signal Process.*, **13**(6), 733 (1994).

Bonvin, D., R. G. Rinker, and D. A. Mellichamp, "Dynamic Analysis and Control of Tubular Autothermal Reactor at an Unstable State," *Chem. Eng. Sci.*, **35**, 603 (1980).

Brown, H. S., I. G. Kevrekidis, and M. S. Jolly, "A Minimal Model for Spatio-Temporal Patterns in a Thin Film Flow," in *Patterns and Dynamics in Reactive Media*, R. Aris, D. Aronson, and H. L Swinney, eds., Springer-Verlag, New York, p. 11 (1991).

Brown, J. R., G. A. D'Netto, and R. A. Schmitz, "Spatial Effects and Oscillations in Heterogeneous Catalytic Systems," in *Temporal Order*, L. Rensing and N. Jaeger, eds., Springer-Verlag, New York, p. 86 (1985).

Brunovsky, P., "Controlling the Dynamics of Scalar Reaction Diffusion Equations by Finite Dimensional Controllers," *Modeling and Inverse Problems of Control for Distributed Parameter Systems*, A. Kurzhanski and I. Lasiecka, eds. Springer Verlag (1991).

Bryson, A. E., and Y. C. Ho, *Applied Optimal Control*, 2nd ed., Blaisdell, Boston (1975).

Canuto, C., M. Y. Hussaini, A. Quarteroni, and T. A. Zang, *Spectral Methods in Fluid Dynamics*, Springer-Verlag, New York (1988).

Carlson, H. A., and J. L. Lumley, "Active Control of the Turbulent Wall Layer in a Minimal Flow Unit," *J. Fluid Mech.*, **329**, 341 (1997).

Chakravarti, S., M. Marek, and W. H. Ray, "Reaction-Diffusion System with Brusselator Kinetics: Control of a Quasiperiodic Route to Chaos," *Phys. Rev. E*, **52**(3), 2407 (1995).

Chang, H.-C., and L.-H. Chen, "Bifurcation Characteristics of Nonlinear Systems Under Conventional PID Control," *Chem. Eng. Sci.*, **39**(7), 1127 (1984).

Chen, C. C., and H.-C. Chang, "Accelerated Disturbance Damping of an Unknown Distributed System by Nonlinear Feedback," *AIChE J.*, **38**(9), 1461 (1992).

Chen, M., and R. Témam, "Nonlinear Galerkin Method in the Finite Difference Case and Wavelet-Like Incremental Unknowns," *Numer. Math.*, **64**, 271 (1993).

Christofides, P. D., and P. Daoutidis, "Nonlinear Control of Diffusion–Convection–Reaction Processes," *Comput. Chem. Eng.*, **20**, S1071 (1996).

Christofides, P. D., and P. Daoutidis, "Finite-Dimensional Control of Parabolic PDE Systems using Approximate Inertial Manifolds," *J. Math. Analy. and Appli.*, **216** 398 (1997).

Christofides, P. D., Robust Control of Parabolic PDE Systems," *Chem. Eng. Sci.*, in press (1998).

Coller, B. D., P. Holmes, and J. L. Lumley, "Control of Noisy Heteroclinic Cycles," *Physica D*, **72**, 135 (1994).

Constantin, P. C., C. Foias, B. Nicolaenko, and R. Témam, *Integral Manifolds and Inertial Manifolds for Dissipative Partial Differential Equations*, Appl. Math. Sci. Ser., Vol. 70, Springer-Verlag, New York (1988).

Cox, A. M., and A. J. Roberts, "Centre Manifolds of Forced Dynamical Systems," *J. Aust. Math. Soc. B*, **32**, 401 (1991).

Curtain, R. F., "Pole Assignment for Distributed Systems by Finite-Dimensional Control," *Automatica*, **21**(1), 57 (1985).

Dainson, B., and M. Sheintuch, "Control of Patterned States," *AIChE J.*, in press (1998).

Deane, A. E., I. G. Kevrekidis, G. Em. Karniadakis, and S. A. Orszag, "Low-Dimensional Models for Complex Geometry Flows: Application to Grooved Channels and Circular Cylinders," *Phys. Fluids*, **3**(10), 2337 (1991).

Doyle, F. J. III, H. M. Budman, and M. Morari, "Linearizing Controller Design for a Packed-Bed Reactor Using a Low-Order Wave Propagation Model," *Ind. Eng. Chem. Res.*, **35**, 3567 (1996).

Erickson, M. A., and A. J. Laub, "An Algorithmic Test for Checking Stability of Feedback Spectral Systems," *Automatica*, **31**(1), 125 (1995).

FitzHugh, R., "Computation of Impulse Initiation and Saltatory Conduction in a Myelinated Nerve Fiber," *Biophys. J.*, **2**(1), 11(1962).

Flaetgen, G., K. Krischer, B. Pettinger, K. Doblhofer, H. Junkes, and G. Ertl, "Two-Dimensional Imaging of Potential Waves on Electrochemical Systems by Surface Plasmon Microscopy," *Science*, **269**, 433 (1988).

Foias, C., and R. Témam, "Algebraic Approximation of Attractors: The Finite Dimensional Case," *Physica D*, **32**, 163 (1988).

Foias, C., M. S. Jolly, I. G. Kevrekidis, G. R. Sell, and E. S. Titi, "On the Computation of Inertial Manifolds," *Phys. Lett. A*, **131**(7,8), 433 (1988a).

Foias, C., G. R. Sell, and R. Témam, "Inertial Manifolds for Nonlinear Evolutionary Equations," *J. Differential Equations*, **73**, 309 (1988b).

Foias, C., and E. S. Titi, "Determining Nodes, Finite Difference Schemes and Inertial Manifolds," *Nonlinearity*, **4**, 135 (1991).

Gay, D. H., and W. H. Ray, "Identification and Control of Distributed Parameter Systems by Means of Singular Value Decomposition," *Chem. Eng. Sci.*, **50**(10), 1519 (1995).

Georgakis, C., R. Aris, and N. R. Amundson, "Studies in the Control of Tubular Reactors, 1-3," *Chem. Eng. Sci.*, **32**, 1359 (1977).

Graham, M., and I. G. Kevrekidis, "Alternative Approaches to Karhunen-Loève Decomposition for Model Reduction and Data Analysis, *Comput. Chem. Eng.*, **20**(5), 495 (1996).

Graham, M. D., P. H. Steen, and E. S. Titi, "Computational Efficiency and Approximate Inertial Manifolds for a Bénard Convection System," *J. Nonlinear Sci.*, **3**, 153 (1993).

Guckenheimer, J., and P. Holmes, *Nonlinear Oscillations, Dynamical Systems and Bifurcations of Vector Fields*, Appl. Math. Sci. Ser., Vol. 42, Springer-Verlag, New York (1983).

Hanczyc, E. M., and A. Palazoglou, "Eigenvalue Inclusion Techniques for Model Approximation to Distributed Parameter Systems," *Ind. Eng. Chem. Res.*, **31**, 2538 (1991).

Hagberg, A., and E. Meron, "Pattern Formation in Non-Gradient Reaction-Diffusion System: The Effect of Front Bifurcations," *Nonlinearity*, **7**, 805 (1994).

Henson, M. A., and D. E. Seborg, eds., *Nonlinear Process Control*, Prentice Hall, Englewood Cliffs, NJ (1996).

Holmes, P., J. L. Lumley, and G. Berkooz, *Turbulence, Coherent Structures, Dynamical Systems and Symmetry*, Cambridge Univ. Press, New York (1996).

Hsu, J. T., and L. Vu-Quoc, "A Rational Formulation of Thermal Circuit Models for Electrothermal Simulation—Part 2: Model Reduction Techniques, *IEEE Trans. Circuits Syst. 1*, **CAS-43**(9), 733 (1996).

Hua, X., M. Magnold, A. Keinle, and E. D. Gilles, "State Profile Estimation of an Autothermal Periodic Fixed-Bed Reactor," *Chem. Eng. Sci.*, **53**(1), 45 (1998).

Imbihl, R., and G. Ertl, "Oscillatory Kinetics in Heterogeneous Catalysis," *Chem. Rev.*, **95**, 697 (1995).

Jauberteau, F., C. Rosier, and R. Témam, "The Nonlinear Galerkin Method in Computational Fluid Mechanics," *Appl. Num. Math.*, **6**, 361 (1989/1990).

Jolly, M. S., I. G. Kevrekidis, and E. S. Titi, "Approximate Inertial Methods for the Kuramoto-Sivashinsky Equation: Analysis and Computations," *Physica D*, **44**, 36 (1990).

Jones, D. A., and E. S. Titi, "A Remark on Quasistationary Approximate Inertial Manifolds for the Navier Stokes Equations," *SIAM J. Math. Anal.*, **25**, 894 (1994).

Joshi, S. S., J. L. Speyer, and J. Kim, "A Systems Theory Approach to the Feedback Stabilization of Infinitesimal and Finite-Amplitude Disturbances in Plane Poiseuille Flow," *J. Fluid Mech.*, **332**, 157 (1997).

Karafyllis, I., P. D. Christofides, and P. Daoutidis, "Dynamical Analysis of a Reaction Diffusion System with Brusselator Kinetics Under Feedback Control," *Proc. Amer. Control Conf.*, p. 2213 (1997).

Kautsky, J., N. K. Nichols, and P. Van Dooren, "Robust Pole Assignment in Linear Feedback," *Int. J. Cont.*, **41**(5), 1129 (1985).

Koda, M., and J. H. Seinfeld, "Reconstruction of Atmospheric Pollutant Concentrations from Remote Sensing Data—An Application of Distributed Parameter Observer Theory," *IEEE Trans. Automat. Contr.*, **AC-27**, 74 (1982).

Kokotovic, P. V., H. K. Khalil, and J. O'Reilly, *Singular Perturbation Methods in Control: Analysis and Design*, Academic Press, New York (1986).

Kokotovic, P. V., and P. W. Sauer, "Integral Manifolds as a Tool for Reduced Order Modeling of Nonlinear Systems: A Synchronous Machine Case Study," *IEEE Trans. Circuits Syst.*, **CAS-36**, 403 (1989).

Kravaris, C., and J. C. Kantor, "Geometric Methods for Nonlinear Process Control," 1-2, *Ind. Eng. Chem. Res.*, **29**, 2295 (1990).

Kunimatsu, N., and H. Sano, "Compensator Design of Semilinear-Parabolic Systems," *Int. J. Control*, **60**(2), 243 (1994).

Kwasniok, F., "Optimal Galerkin Approximations of Partial Differential Equations Using Principal Interaction Patterns," *Phys. Rev. E*, **35**, 5365 (1997).

Liauw, M. A., M. Somani, and D. Luss, "Oscillating Temperature Pulses During CO Oxidation on a $Pd/Al_2O_3$ Ring," *AIChE J.*, **43**(6), 1519 (1997).

Loffler, H. P., and W. Marquardt, "On the Order Reduction of Nonlinear Differential-Algebraic Process Models," *Proc. ACC*, 1546 (1992).

Lorenz, E. N., "Empirical Orthogonal Functions and Statistical Weather Prediction," Tech. Rep. 1, MIT, Dept. of Meteorology Statistical Forecasting Project, Cambridge, MA (1956).

Marion, M., and R. Témam, "Nonlinear Galerkin Methods: The Finite Element Case," *Numer. Math.*, **57**, 205 (1990).

Marquardt, W., and H. Auracher, "An Observer Based Solution of Inverse Heat Conduction Problems," *Int. J. Heat Mass Transfer*, **33**, 1545 (1990).

McDermott, P. E., and H.-C. Chang, "On the Global Dynamics of an Autothermal Reactor Stabilized by Linear Feedback Control," *Chem. Eng. Sci.*, **51**(1), 1347 (1984).

Meadows, E. S., and J. B. Rawlings, "Model Predictive Control," in *Nonlinear Process Control*, M. A. Henson and D. E. Seborg, eds., Prentice Hall, Englewood Cliffs, NJ (1994).

Nieken, U., G. Kolios, and G. Eigenberger, "Control of the Ignited Steady State in an Autothermal Fixed-Bed Reactor for Catalytic Combustion," *Chem. Eng. Sci.*, **59**, 5509 (1994).

Ogunnaike, B. A., and W. H. Ray, *Process Dynamics, Modeling and Control*, Oxford Univ. Press, New York (1994).

Paduano, J. D., L. Valavani, A. H. Epstein, E. M. Greitzer, and G. R. Guenette, "Modeling for Control of Rotating Stall," *Automatica*, **30**(9), 1357 (1994).

Park, H. M., and D. H. Cho, "The Use of Karhunen-Loève Decomposition for the Modeling of Distributed Parameter Systems," *Chem. Eng. Sci.*, **51**(1), 81 (1996).

Petrov, V., Q. Ouyang, and H. L. Swinney, "Resonant Pattern Formation in a Chemical System," *Nature*, **388**, 655 (1997).

Qin, F., and E. E. Wolf, "Vibrational Control of Chaotic Self-Sustained Oscillations during CO Oxidation on $Rh - Al_2O_3$ Catalyst," *Chem. Eng. Sci.*, **50**(1), 117 (1995).

Qin, F., and E. E. Wolf, "Spatially Resolved Infrared Spectroscopy: A Novel Technique for *in situ* Study of Spatial Surface Coverage During CO Oxidation on Supported Catalysts," *Catal. Lett.*, **39**, 19 (1996).

Ray, W. H., *Advanced Process Control*, McGraw-Hill, New York (1981).

Rigopoulos, A., Y. Arkun, and F. Kayihan, "Identification of Full Profile Disturbance Models for Sheet Forming Processes," *AIChE J.*, **43**(3), 727 (1997).

Rotermund, H. H., W. Engel, M. E. Kordesch, and G. Ertl, "Imaging Spatiotemporal Pattern Evolution during Carbon Monoxide Oxidation on Platinum," *Nature*, **343**, 355 (1990).

Russell, R. D., D. M. Sloan, and M. R. Trummer, "Some Numerical Aspects of Computing Inertial Manifolds," *SIAM J. Sci. Stat. Comput.*, **14**(1), 19 (1993).

Sahan, R. A., A. Liakopoulos, and H. Gunes, "Reduced Dynamical Models of Nonisothermal Transitional Grooved Channel Flow," *Phys. Fluids*, **9**(3), 551 (1997).

Sakawa, Y., "Feedback Stabilization of Linear Diffusion Systems," *SIAM J. Control Optim.*, **21**(5), 667 (1983).

Sano, H., and N. Kunimatsu, "Feedback Control of Semilinear Diffusion Systems: Inertial Manifolds for Closed-Loop Systems, *IMA J. Math. Control Informat.*, **11**, 75 (1994).

Sheintuch, M., and S. Shvartsman, "Spatiotemporal Patterns in Catalytic Reactors," *AIChE J.*, **42**(4), 1041 (1996).

Shen, J., and R. Témam, "Nonlinear Galerkin Method Using Chebyshev and Legendre Polynomials 1. The One-Dimensional Case," *SIAM J. Numer. Anal.*, **32**(1), 215 (1995).
Sirovich, L., and J. D. Rodriguez, "Coherent Structures and Chaos: A Model Problem," *Phys. Lett. A*, **120**(5), 211 (1989).
Sirovich, L., W. B. Knight, and J. D. Rodriguez, "Optimal Low-Dimensional Dynamical Approximations," *Q. Appl. Math.*, **48**(3), 555 (1990).
Somani, M., M. A. Liauw, and D. Luss, "Hot Spot Formation on a Catalyst," *Chem. Eng. Sci.*, **51**, (1996).
Su, T., and R. R. Craig, Jr., "Model Reduction and Control of Flexible Structures Using Krylov Vectors," *J. Guid. Control Dyn.*, **14**(2) (1991).
Témam, R., "Infinite Dimensional Dynamical Systems in Mechanics and Physics," *Appl. Math. Sci. Ser.*, Vol. 68, Springer-Verlag, New York (1988).

*Manuscript received Nov. 17, 1997, and revision received Apr. 8, 1998.*